Construction and Building Materials 172 (2018) 660–669

Contents lists available at ScienceDirect

Construction and Building Materials

journal homepage: www.elsevier.com/locate/conbuildmat

Mechanical properties and constitutive equations of crumb rubber mortars

Wei-Jie Song [a,b], Wei-Guo Qiao [a,b,*], Xu-Xu Yang [a,b], Deng-Ge Lin [a,b], Yan-Zhi Li [a,b]

[a] Shandong Provincial Key Laboratory of Civil Engineering Disaster Prevention and Mitigation, Shandong University of Science and Technology, Qingdao 266590, China
[b] College of Civil Engineering and Architecture, Shandong University of Science and Technology, Qingdao 266590, China

HIGHLIGHTS

- A series of triaxial tests were implemented to exam the mechanical behavior of crumb rubber mortars.
- The necessity of incorporating the influence of the damage threshold into the damage evolution model was discussed.
- A damage constitutive model of crumb rubber mortars was established.

ARTICLE INFO

Article history:
Received 4 November 2017
Received in revised form 14 March 2018
Accepted 29 March 2018

Keywords:
Crumb rubber mortars
Damage threshold
Microcosmic element strength
Constitutive model
Strain softening

ABSTRACT

There will be a lot of pollution in the process of production and degradation of rubber. It is imperative to recycle rubber in order to build a green and saving environment. A new kind of mortar with rubber particles is an effective way to reuse the used rubber products. The crumb rubber mortar effectively resist external stress through its own deformation. Therefore, it is of practical significance to study the strength behavior of crumb rubber mortar. The stress-strain curves of crumb rubber mortars with 5 different rubber contents under a triaxial stress condition are obtained through laboratory testing. The internal variation law of the elastic modulus, Poisson's ratio and damage variable are analyzed, and the necessity of incorporating the influence of the damage threshold into the damage evolution model is discussed. According to a rock damage model based on Lemaitre's strain equivalence theory and the introduction of the damage threshold based on the traditional Weibull random distribution, the damage constitutive model of crumb rubber mortars under the influence of the damage threshold is established by considering two factors. The method of determining the model parameters is presented. The model can describe the entire process of strain softening and deformation of crumb rubber mortars for various levels of rubber content or confining pressure. The model can also fully reflect the linear elastic deformation characteristics of rock under small deformations and the nonlinear mechanical behavior after the peak strength is exceeded. The model is particularly suitable for describing the complex stress states in the field of underground engineering, and it provides a reference for the design of supporting structures. Finally, by comparing the measured results of three-axis compression tests of crumb rubber mortars with various rubber contents, the rationality of the model is verified.

1. Introduction

With the rapid development of the global transportation industry, the number of used automobile tires has increased dramatically. Rubber, the main component of tires, features a strong thermal degradation resistance; thus, the efficient recycling of waste rubber has become a scientific and engineering challenge that requires urgent solution [1,2]. In 2015, countries at the Paris Climate Conference agreed on an energy consumption and carbon emission reduction strategy and advocated policies to conserve resources and protect the environment. At present, the civil engineering materials industry is focused on the efficient use of renewable materials and has advocated for green development. To effectively improve the physical and mechanical properties of mortars and improve its ductility and compressive deformation capacity, rubber particles can be effectively combined with cement and sand to form crumb rubber mortars. In this way, resources can

* Corresponding author at: Shandong Provincial Key Laboratory of Civil Engineering Disaster Prevention and Mitigation, Shandong University of Science and Technology, Qingdao 266590, China.
E-mail address: Qiaowg1@163.com (W.-G. Qiao).

https://doi.org/10.1016/j.conbuildmat.2018.03.263
0950-0618/

be recycled to promote the sustainable development of nature, the economy and society in general. Therefore, it is necessary to systematically study the mechanical properties of crumb rubber mortars [3–5].

Crumb rubber mortars have been widely used in the fields of building construction, road construction and underground engineering. In particular, crumb rubber mortars can be introduced into highways, high-speed railways, and airport pavements. Furthermore, crumb rubber mortars have been used as a structural material to enhance the dynamic performance and seismic performance of concrete structures [6,7]. Scholars worldwide have conducted substantial experimental research on the mechanical properties and durability of crumb rubber mortars and have achieved a series of valuable results [8–10]. For example, Li et al. used various content and sizes of rubber particles filling high-strength concrete (RHSC) to conduct mechanical experimental research [11]. The results showed that adding rubber powder can reduce the strength of high-strength concrete, increase energy absorption capacity, reduce brittleness, and increase the ductility of high-strength concrete. Shen et al. used scanning electron microscope (SEM) to observe polymer–rubber aggregate-modified porous concrete [12]. Their study found that the interfacial transition zones between the rubber and cement slurry were enhanced by the polymer and that the polymer films in the cement hydrate and rubber particles lay in a staggered distribution, increasing the flexibility of the crumb rubber concrete (CRC). By changing the volume ratio of the rubber particles in crumb rubber mortars, Khaloo et al. found that the brittle behavior of rubber granule concrete decreases as the rubber content increases and that its strength and tangential elastic modulus are greatly reduced [13]. Liu et al. studied the fatigue properties of standard crumb rubber mortar samples with 60 different rubber contents [14]. The results showed that under certain stress levels, the fatigue life and dynamic strain of crumb rubber mortars are higher than that of ordinary concrete. Li et al. conducted uniaxial compression tests on rubber concrete (RC) with various rubber volume contents and particle sizes [15]. A uniaxial compression constitutive model of low volume RC was established and optimized. Zhang et al. used acrylic acid (ACA) and polyethylene glycol (PEG) to treat rubber particles [16]. The results showed that relative to unmodified RC, the compressive and flexural strengths of modified rubberized concrete (MRC) with 10% rubber particle content can be increased by 25.9% and 26.4%, respectively. Su et al. used concrete particles of various particle sizes in concrete instead of 20% of natural fine aggregate in volume [17]. The results showed that rubber aggregates with smaller or continuously graded size have relatively high strengths and low water permeabilities. Feng et al. conducted uniaxial compression tests on CRC [18]. The experimental results showed that the uniaxial compressive strength of CRC decreases as the colloidal rubber content increases, and a formula for the estimation of CRC strength was also proposed. Osório et al. [19,20] analyzed the effect of rubber content on the mechanical properties and porosity of cement mortars and focused on the interrelation of strength/porosity in the rubberized cement and mortars. Through SEM micrographs of the fractured surface of the rubberized cement mortar, spheroidal and irregular porous morphologies were clearly observed.

By analyzing the above documents, research on RC focuses on strength, brittleness and durability. Research on the mechanical properties and constitutive model of crumb rubber mortars is relatively limited and confined to uniaxial compression at present. However, in the field of underground engineering, crumb rubber mortars as a support structure are often placed under a triaxial stress state. Therefore, to determine whether crumb rubber mortars can be used as a structural material, it is important to determine the stress-strain relation of crumb rubber mortars under the triaxial stress state.

In this paper, a series of triaxial tests have been carried out to exam the strength and deformation behavior of crumb rubber mortars with 5 different rubber proportions. The necessity of incorporating the influence of the damage threshold into the damage evolution model has been discussed. Moreover, a constitutive model of triaxial compression for crumb rubber mortars has been proposed that can be used to predict their stress-strain response. And the method for determining parameters of the constitutive model is also described. Through comparison with the experimental results, the rationality of the model was verified. This study is intended to promote the application of crumb rubber mortars in underground engineering stabilization.

2. Experimental study of physical mechanics

2.1. Materials and mixing ratio

The chemical composition and physical and mechanical properties of P.O42.5-grade Portland cement produced in Ji'nan are shown in Tables 1 and 2. The fine aggregate includes sand and rubber particles. The sand used is local river sand, with a maximum particle size of 5 mm and a continuous gradation. The particle size of the rubber is 6–8 mm, and the apparent density is 1200 g/cm^3. Recycled used rubber products were pre-treated, including sorting, removal of impurities, cutting, cleaning, drying and other processing procedures. In the end, rubber particles with pure color, uniform particles, and qualified technical indicators were selected as test materials. Additives include a water reducer and binders. The water reducer is naphthalene-reducing superplasticizer DC-WR1 with a water-reducing rate of 15%–25%, with the appearance of yellowish brown powder. The binder adopted DC-W10 polyacrylate emulsion. The test water is ordinary tap water. The specific experimental materials are shown in Fig. 1.

A mixing ratio of M-0% is used as the control group, the ratio of water to cement (W/C) is 0.35, and the ratio of sand to cement (S/C)

Table 1
Chemical composition of P.O42.5-grade ordinary Portland cement.

CaO	SiO_2	Al_2O_3	Fe_2O_3	SO_3	MgO	Na_2O	K_2O	Ignition Loss
63.57	20.97	5.21	5.03	2.18	1.31	0.35	0.13	1.25

Table 2
Physical and mechanical properties of P.O42.5-grade ordinary Portland cement.

Specific surface area (cm^2/g)	Density (g/cm^3)	Setting time		Compressive strength (MPa)	Flexural strength (MPa)
		Initial (min)	Final (min)		
3450 ± 50	3.00 ± 0.02	120 ± 5	310 ± 10	48.5 ± 2.0	9.2 ± 0.5

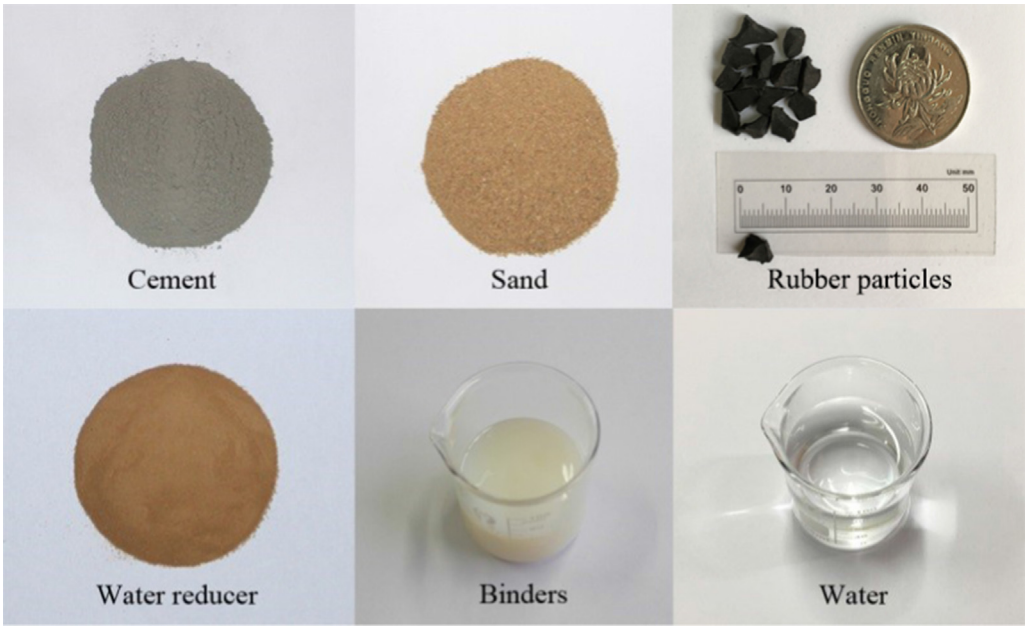

Fig. 1. Test materials: cement, sand, rubber particles, water reducer, binders and water.

Table 3
Mortar mixture proportions (by weight).

Mix	Cement	Sand	Rubber particles	Water reducer	Binders	Water
M-0%	1	1.5	0	0.015	0	0.35
M-5%	1	1.5	0.152	0.015	0.023	0.35
M-10%	1	1.5	0.324	0.015	0.049	0.35
M-15%	1	1.5	0.519	0.015	0.078	0.35
M-20%	1	1.5	0.744	0.015	0.112	0.35

Note: the error range for weight proportion values in this table is ±0.001.

is 1.5. The rubber particles are introduced into the mortar mixture at various mass ratios (0%, 5%, 10%, 15%, 20%); the mixing ratio of the crumb rubber mortars is shown in Table 3. Taking into account the mixing ratio of rubber particles, the mortar mixture is specified, making it easy to reference. For example, a mixture specification of M-10% means that the mass of the rubber particles is 10% of the total mass of the mixture of crumb rubber mortars.

2.2. Sample preparation and test methods

Five groups of rubber particle mortars specimens are designed in this experiment. Each group contains 9 specimens, and the total number of specimens is 45. The specimen is a Φ50 mm × 100 mm cylinder. The samples were molded and demolished after 24 h. They were maintained for 28 d at laboratory temperatures of 20 °C ± 2 °C and a relative humidity of 95% RH. The cross section diagram of the rubber particle mortars sample and the locally magnified drawing diagram obtained through the test are shown in Fig. 2. Then, an MTS rock servo test machine was used to conduct uniaxial and three-axis compression tests. The loading process was controlled by displacement, the load speed is 0.1 mm/min. In order to ensure repeatability of test, 3 same rubber particle mortar specimens were tested repeatedly in the same stress state in each group. The experimental operation process is based on Chinese standards (GB/T 50266-1999 for rock mass test methods and GB/T 50081-2002 for standard test methods of the mechanical properties of ordinary concrete).

2.3. Results and discussion

By averaging the results of 3 tests in each group, the stress-strain curves of crumb rubber mortars with various rubber contents under various confining pressures are shown in Fig. 3. The strength of the crumb rubber mortars increases with the confining pressure for samples with the same rubber particle content. When the peak strength is reached, the crumb rubber mortars gradually transition from brittle to ductile, and the softening characteristics of the rock plastic strain decrease gradually. Under the same confining pressure, the strength of crumb rubber mortars decreases gradually as the rubber particle content increases. The gap between the peak strength and the residual strength gradually decreases, and the crumb rubber mortars gradually exhibit ideal plasticity characteristics. Further analysis shows that the elastic modulus, E, and Poisson's ratio, μ, of crumb rubber mortars also exhibits a characteristic response. Through data fitting of the elastic modulus of mortars with various rubber particle contents, the following relationship is observed, as shown in Fig. 4.

$$E = -0.60M^3 + 29.75M^2 - 509.70M + 4068.47 \quad (1)$$

Here, M is the percentage value of the rubber particle content, i.e., the amount of rubber in the samples is M%.

By analyzing the radial and axial strains of the experimental data, it is found that the Poisson's ratio, μ, of crumb rubber mortars changes approximately linearly with the axial strain, ε_1, before the peak strain. After the peak strain, Poisson's ratio, μ, increases

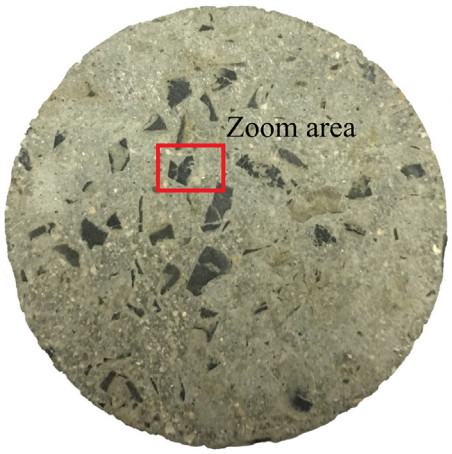

(a) The cross section diagram of the rubber particle mortars sample.

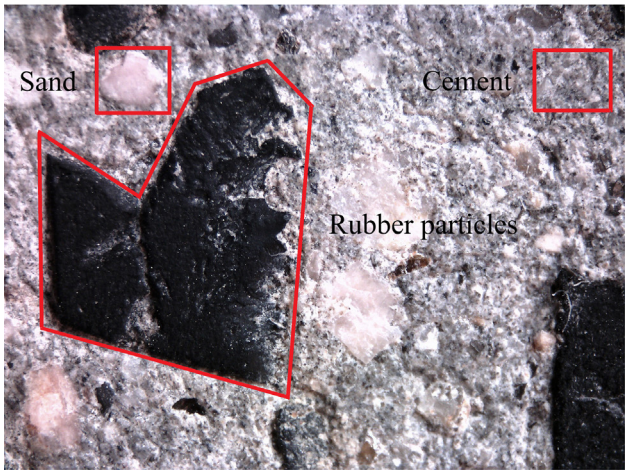

(b) The locally magnified drawing diagram of the rubber particle mortars sample.

Fig. 2. The cross section diagram of the rubber particle mortars sample and the locally magnified drawing diagram.

slowly with increasing axial strain, ε_1. Further analysis shows that the ratio conforms to the changing law of a logarithmic function. Therefore, it is assumed that Poisson's ratio, μ, is related to the axial strain, ε_1, as follows:

$$\mu = \begin{cases} A\varepsilon_1, (\varepsilon_1 \leqslant \varepsilon_{pk}) \\ B\ln\varepsilon_1 + C, (\varepsilon_1 > \varepsilon_{pk}) \end{cases} \quad (2)$$

here A is determined by the peak axial strain, ε_{pk}, and the peak Poisson's ratio, μ. B and C require two sets of data to determine. The first set of data is taken from the vicinity of the initial load, and it is assumed that when a = 0.001, then c = 0.001. The second set of data is taken from the peak.

According to the Poisson's ratio, μ, calculated using Eq. (2), the axial strain–radial strain curve under theoretical conditions is obtained, which is compared with the data obtained under the experimental conditions as shown in Fig. 5. For example, Exp-0 and Fit-0 refer to the data of crumb rubber mortar samples obtained through the experiment at a confining pressure of 0 MPa and are obtained by fitting the parameters at a confining pressure of 0 MPa. As shown in Fig. 5, the theoretical fit of Poisson's ratio is in good agreement with the experimental data at the initial deformation stage, but errors appear in the late deformation stage. These errors are all limited to a reasonable range, however. As a whole, the results of fitting the Poisson's ratio can accurately describe the experimental data.

3. Establishment of the constitutive model

3.1. The change law of damage factors

The entire process of compressive deformation of crumb rubber mortars can be divided into an elastic stage (OA segment), plastic deformation stage (AB segment) and failure stage (BC segment), as shown in Fig. 6. In the elastic stage, the stress-strain curve of the crumb rubber mortars is linear, and the elastic modulus is constant. That is, the crumb rubber mortars do not cause damage during the deformation stage [21].

The above rock deformation process is actually a continuous damage process of rock under loading. Generally, the damage model based on the Lemaitre strain equivalence assumption is used to describe the process [22], i.e.,

$$\sigma_i = \sigma_i'(1 - D) \quad (3)$$

where σ_i and σ_i' are the macroscopic nominal stress and microscopic stress of the undamaged part of the rock, respectively, and D is the damage factor. Since σ_i' is the microscopic stress of the undamaged parts of the rock, it can be assumed that its deformation obeys the linear elastic Hooke's law:

$$\sigma_i' = E\varepsilon_i' + \mu'(\sigma_j' + \sigma_k') \quad (4)$$

where i, j, and k = 1, 2, and 3, respectively; ε_i' is the microscopic strain of the undamaged parts of the rock, and μ' is the Poisson's ratio of the undamaged material in the rock. According to the deformation compatibility condition of the damaged and undamaged materials in the rock, the following results can be obtained:

$$\varepsilon_i' = \varepsilon_i \quad (5)$$

here ε_i is the macro strain of the rock. The Poisson's ratio, μ, of the rock and the Poisson's ratio, μ', of the undamaged part of the rock can be obtained using the physical interpretation of the Poisson's ratio of the material. The results are as follows:

$$\mu = |\varepsilon_3/\varepsilon_1| \quad (6)$$

$$\mu' = |\varepsilon_3'/\varepsilon_1'| \quad (7)$$

Thus, the following result can be obtained using Eqs. (5)–(7):

$$\mu = \mu' \quad (8)$$

We substitute Eq. (8) into Eq. (4), and the following result can be obtained by combining Eqs. (3) and (5):

$$\sigma_i = E\varepsilon_i(1 - D) + \mu(\sigma_j + \sigma_k) \quad (9)$$

This equation is the damage model that describes the process of rock strain softening deformation.

To establish a more realistic model of rock damage evolution, it is necessary to discuss the change law of the rock damage variable with the test curve to understand the value of the rock damage variable or damage factor [23]. For this reason, the following equation is obtained by transforming Eq. (9):

$$D = [E\varepsilon_1 - \sigma_1 - \mu(\sigma_2 + \sigma_3]/(E\varepsilon_1) \quad (10)$$

The D-ε_1 curves are obtained using the σ_1 values and ε_1 values of each measuring point in the stress-strain curve obtained by laboratory testing and Eq. (10). The D-ε_1 curve is shown in Fig. 7.

When the axial deformation is small (for the example in this study, ε_1 is less than approximately 0.005), the damage factor is generally 0.6–12. In addition, $D < 0$ in some cases. This result is not consistent with a reasonable range of the damage factor (0 ≤

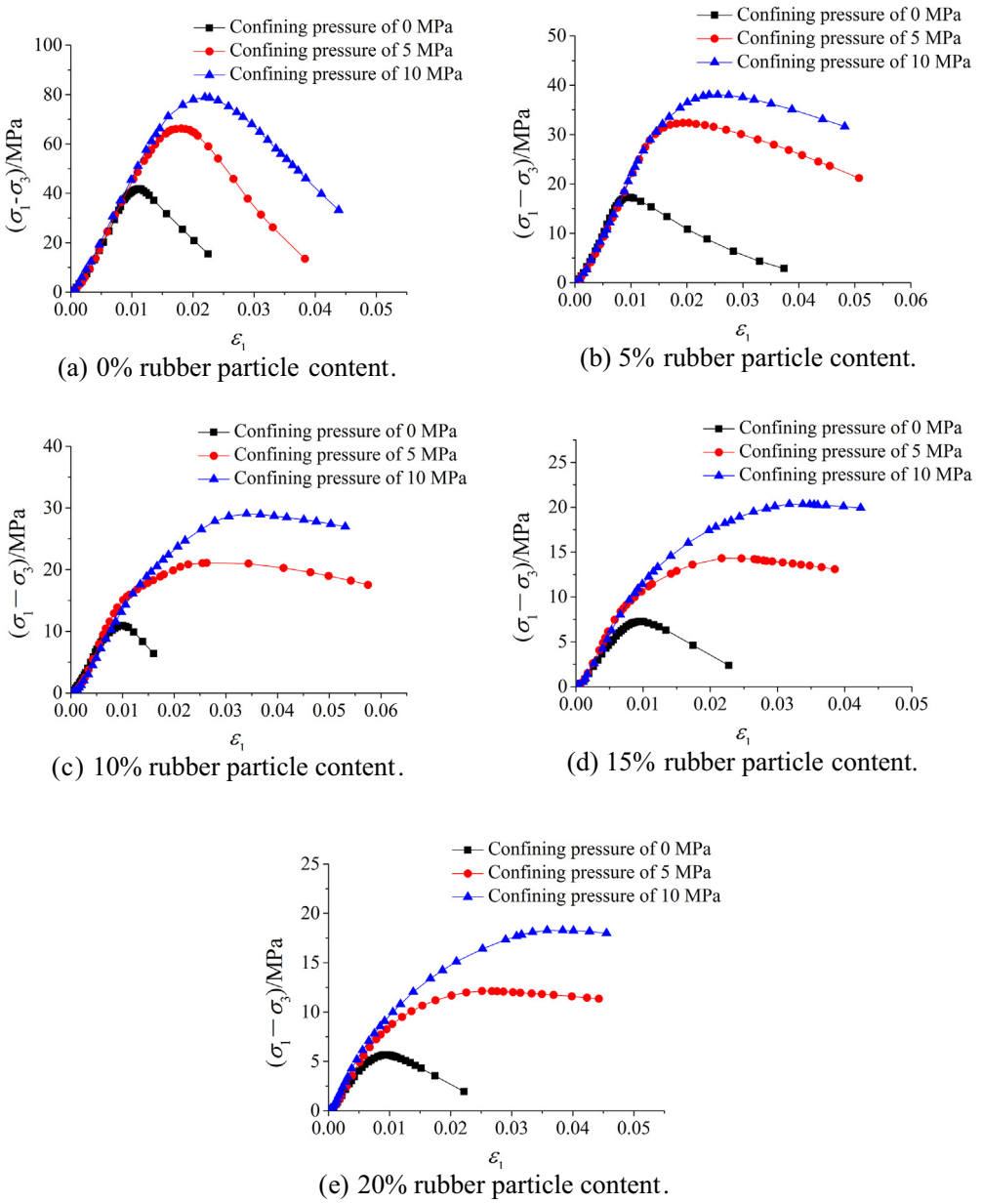

Fig. 3. Stress-strain curves of crumb rubber mortars with various rubber particle contents under conventional triaxial compression.

$D \leq 1$) and the range of values. No damage can occur on the crumb rubber mortars during the elastic stage (as shown in Fig. 7). The damage factor, D, of mortars should be constant at 0, which shows

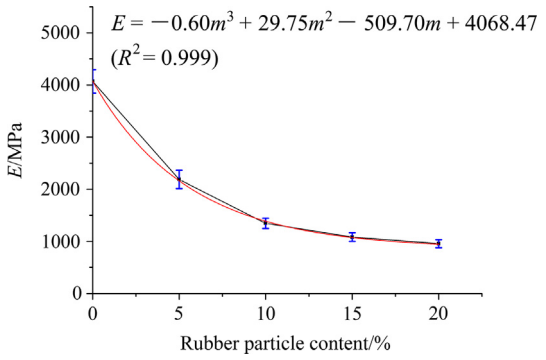

Fig. 4. Relationship between rubber particle content and the elastic modulus of crumb rubber mortars.

the influence of the damage threshold of mortars. This condition explains the influence of the damage threshold of crumb rubber mortars. When the deformation of crumb rubber mortars is large (for example, when ε_1 is more than approximately 0.005), the damage variable or damage factor is always in the range of [0, 1], which is reasonable.

Thus, a threshold problem exists for crumb rubber mortars. The damage mechanism and characteristics of crumb rubber mortars noted above must be reflected when the damage constitutive model of crumb rubber mortars is established.

3.2. Establishment of the constitutive model and the method of parameter determination

A single element is taken in any cross section of the crumb rubber mortar specimen under uniaxial or triaxial compression. Although we assume that the element size is sufficiently large to contain many microscopic cracks and microscopic voids, it is also sufficiently small to remain compatible with continuum damage

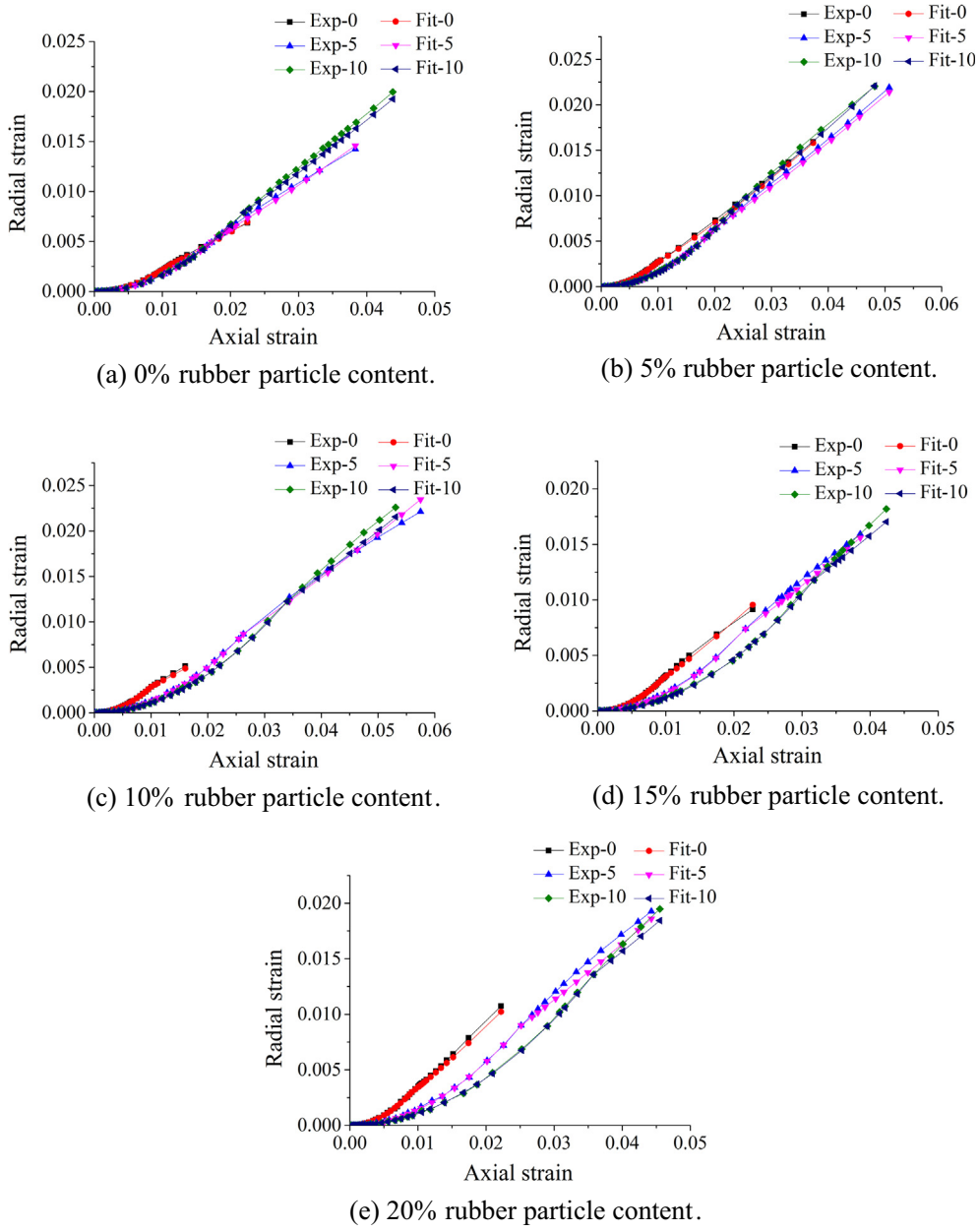

Fig. 5. Relationship between the axial strain and radial strain of crumb rubber mortars with various rubber particle contents.

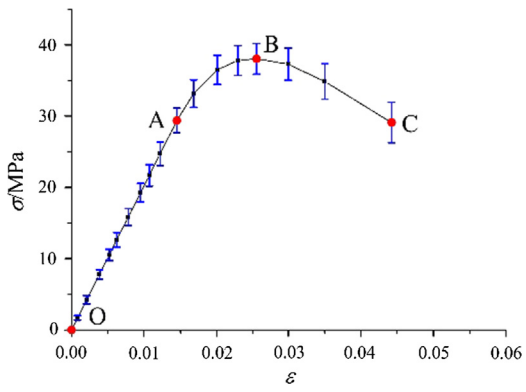

Fig. 6. The complete process of compression deformation of crumb rubber mortars.

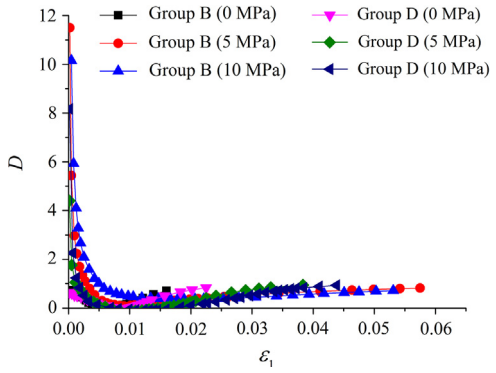

Fig. 7. Relationship between the axial strain and damage factor of crumb rubber mortars with various rubber particle contents.

mechanics. That is, we assume that the CRC exhibits a continuous distribution, as discussed previously [24]. Therefore, we hypothesize that 1) the micro-element obeys generalized Hooke's law, 2) the damage of the micro-element conforms to the Mises yield criterion, and 3) the intensity of the micro-element is randomly drawn from the Weibull distribution [25–27].

$$\left.\begin{aligned} D &= \int_0^k \Phi(x)\mathrm{d}x = 0, (\varepsilon < k) \\ D &= \int_k^\varepsilon \Phi(x)\mathrm{d}x = 1 - \exp\left[-\left(\frac{\varepsilon-k}{a}\right)^m\right], (\varepsilon \geqslant k) \end{aligned}\right\} \tag{11}$$

In Eq. (11) [28,29], ε is the strain, m is the shape parameter, and a is the scale parameter. These values are nonnegative. On this basis, the damage threshold parameter k is introduced as above.

In this way, the damage variable is consistent with the three-stage characteristics of the complete process of the compressive deformation of crumb rubber mortars as shown in Fig. 6. Substituting Eq. (11) into Eq. (9), we obtain the following results:

$$\sigma = \begin{cases} E\varepsilon + \mu(\sigma_2 + \sigma_3), (\varepsilon < k) \\ E\varepsilon \exp\left[-\left(\frac{\varepsilon-k}{a}\right)^m\right] + \mu(\sigma_2 + \sigma_3), (\varepsilon \geqslant k) \end{cases} \tag{12}$$

The following geometric boundary conditions are determined from the full stress-strain curve [28]: ① $\varepsilon = 0$, and $\sigma = 0$. ② $\varepsilon = 0$, and $\frac{\mathrm{d}\sigma}{\mathrm{d}\varepsilon} = E$. ③ $\sigma = \sigma_{pk}$, and $\varepsilon = \varepsilon_{pk}$. ④ $\sigma = \sigma_{pk}$, and $\frac{\mathrm{d}\sigma}{\mathrm{d}\varepsilon} = 0$, as shown in Fig. 8.

For the derivation of the strain of the second type in Eq. (12), the following can be written:

$$\frac{\mathrm{d}\sigma}{\mathrm{d}\varepsilon} = E\exp\left[-\left(\frac{\varepsilon-k}{a}\right)^m\right]\left(1 - \frac{m\varepsilon}{(\varepsilon-k)}\left(\frac{\varepsilon-k}{a}\right)^m\right) \tag{13}$$

Boundaries ① and ② are in full compliance with the above conditions. Substituting condition ③ into the second equation in Eq. (12) and substituting condition ④ into Eq. (13), we obtain the following:

$$\left.\begin{aligned} &\sigma_{pk} = E\varepsilon_{pk}\exp\left[-\left(\frac{\varepsilon_{pk}-k}{a}\right)^m\right] + \mu(\sigma_2 + \sigma_3) \\ &E\exp\left[-\left(\frac{\varepsilon_{pk}-k}{a}\right)^m\right]\left[1 - \frac{m\varepsilon_{pk}}{(\varepsilon_{pk}-k)}\left(\frac{\varepsilon_{pk}-k}{a}\right)^m\right] = 0 \end{aligned}\right\} \tag{14}$$

In Eq. (14), ε_{pk} and σ_{pk} are the peak strain and peak stress under the uniaxial or triaxial load, respectively.

From Eq. (14), $E \neq 0$ in the second formula, and $\exp\left[-\left(\frac{\varepsilon_{pk}-k}{a}\right)^m\right] \neq 0$; the following result can be obtained:

$$1 - \frac{m\varepsilon_{pk}}{\varepsilon_{pk}-k}\left(\frac{\varepsilon_{pk}-k}{a}\right)^m = 0 \tag{15}$$

Substituting Eq. (15) into the first equation in Eq. (14), we obtain

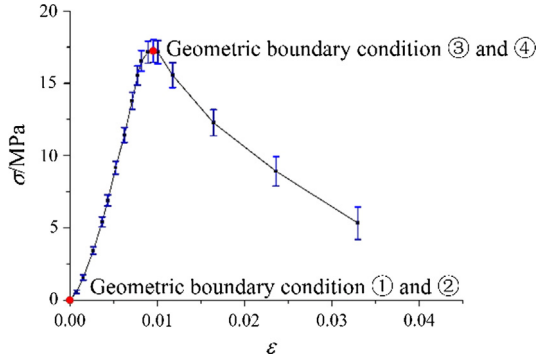

Fig. 8. Geometrical boundary conditions of the complete stress-strain curve.

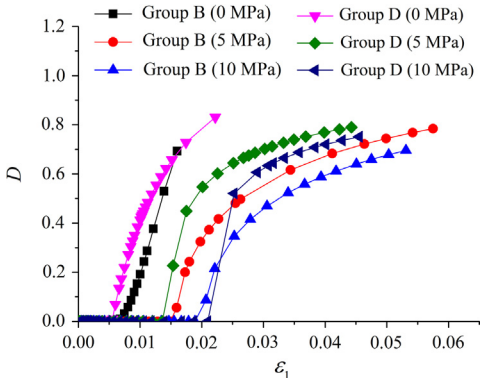

Fig. 9. Theoretical curves of D-ε_1 of crumb rubber mortars in group B and D with the confining pressure of 5 MPa.

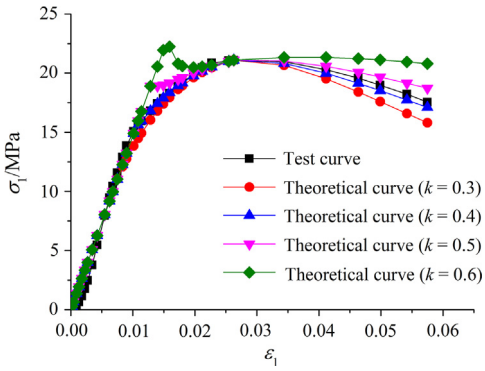

Fig. 10. Comparison of theoretical curves with experimental curves under different k values.

$$m = \frac{\varepsilon_{pk} - k}{\varepsilon_{pk}} \frac{1}{\ln\frac{E\varepsilon_{pk}}{\sigma_{pk} - \mu(\sigma_2+\sigma_3)}} \tag{16}$$

Then, the following results can be obtained from Eq. (15):

$$a = \frac{\varepsilon_{pk} - k}{\left(\frac{\varepsilon_{pk}-k}{m\varepsilon_{pk}}\right)^{\frac{1}{m}}} \tag{17}$$

When k is taken as a fixed value, the unknown model parameters of Eq. (12) are all obtained. Thus, the damage constitutive model of crumb rubber mortars considering the damage threshold is established. Using the equations, E, ε_{pk}, σ_{pk}, a and m can be determined from the experimental results.

4. Analysis and discussion

The parameters m and a are determined by substituting the experimental data into Eqs. (16) and (17). Then, the parameters m and a are substituted into Eq. (11) to obtain the parameters of the damage variable or the damage factor. If the damage threshold parameter is taken as $k = 0.6\varepsilon_{pk}$, then Fig. 9 is obtained. In contrast to the behavior shown in Fig. 9 and Fig. 7, the damage variable can reflect the three stages of compression deformation of crumb rubber mortars shown in Fig. 3 through the damage constitutive model established by considering the influence of the damage threshold.

The two parameters m and a in the constitutive model are determined by expressions and have well-defined physical meanings. The damage threshold parameter k is determined by the

Table 4
k' values and k'' values of crumb rubber mortars with different rubber particle content.

Mix	Confining pressure/MPa	k'	k''
M-0%	0	0.89	0.880
	5	0.75	0.756
	10	0.65	0.632
M-5%	0	0.75	0.740
	5	0.60	0.616
	10	0.49	0.492
M-10%	0	0.60	0.600
	5	0.45	0.476
	10	0.34	0.352
M-15%	0	0.44	0.460
	5	0.30	0.336
	10	0.20	0.212
M-20%	0	0.34	0.320
	5	0.20	0.196
	10	0.10	0.072

properties of the different materials. Therefore, the influence of the damage threshold parameter, k, on the constitutive model is discussed here. The change rule of the damage parameter, k, of crumb rubber mortars under various confining pressure conditions is determined, which augments the constitutive model. Taking M-10% crumb rubber mortars as an example, the confining pressure is 5 MPa. Based on the damage statistical constitutive model of crumb rubber mortars established in this model, various damage threshold parameters, k, are determined. The theoretical curves of stress-strain curves are obtained and compared with the experimental curves, as shown in Fig. 10.

When the damage threshold, k, is 0.4 ε_{pk}, the test curve can be more accurately described than the conditions for which k is 0.3 ε_{pk}, 0.5 ε_{pk} or 0.6 ε_{pk}. Thus, the optimum damage threshold k' of crumb rubber mortars under various contents and confining pressure conditions can be determined. Linear fitting is achieved by obtaining the best damage threshold, k'. The relationship between

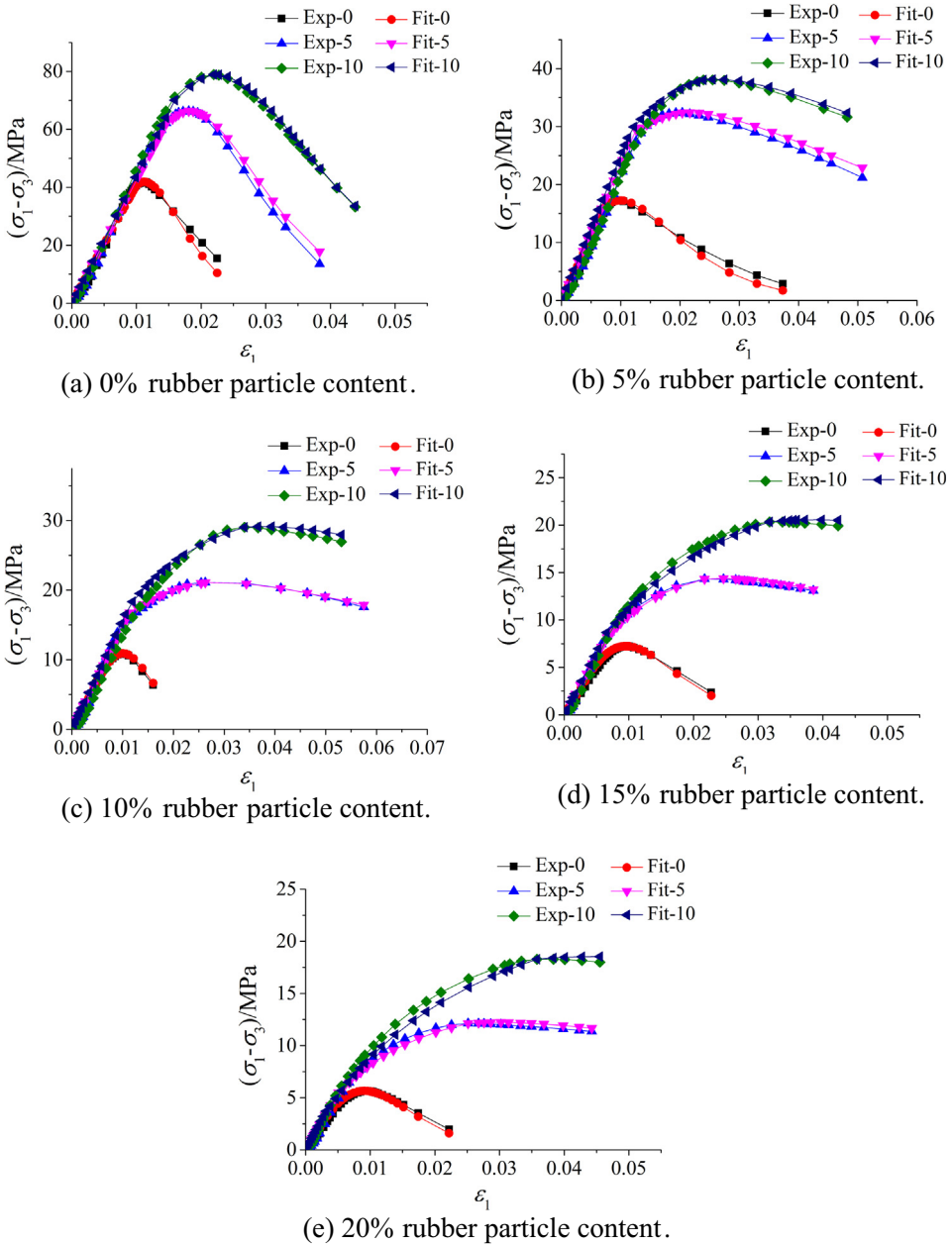

(a) 0% rubber particle content.
(b) 5% rubber particle content.
(c) 10% rubber particle content.
(d) 15% rubber particle content.
(e) 20% rubber particle content.

Fig. 11. Comparison between the experimental and theoretical curves.

the optimum damage threshold, k', and the rubber particle content, $m\%$, and the confining pressure, σ_3, is as follows:

$$K' = -0.0248\sigma_3 + (-0.028M + 0.88) \tag{18}$$

The goodness of fit of this equation is greater than 0.99. Therefore, the optimum damage threshold, k', is accurately determined. To better distinguish the variables, the damage threshold calculated for this equation is defined as the fitting damage threshold, k''. The optimum damage threshold, k', and the fitting damage threshold, k'', are shown in Table 4.

As the rubber particles in the crumb rubber mortars increase in concentration, the damage threshold, k, is gradually reduced. Thus, as the rubber particle content increases, the space of coarse aggregates (such as sand) decreases gradually in crumb rubber mortars, increasing the material's susceptibility to damage. In addition, as confining pressure increases, the damage threshold, k, gradually decreases. The confining pressure increases the strength and limits the radial deformation while reducing the damage threshold of crumb rubber mortars. When the confining pressure increases from 0 MPa to 5 MPa, the damage threshold decreases by approximately 0.15. When the confining pressure increases from 5 MPa to 10 MPa, the damage threshold decreases by approximately 0.10. For the damage threshold, the latter changes less with respect to the former. The variation law of k' values and k'' values in Table 4 tends to be generally consistent; thus, the value of the damage threshold k is reasonable.

$$\sigma = \begin{cases} E\varepsilon + \mu(\sigma_2 + \sigma_3), (\varepsilon < k'') \\ E\varepsilon \exp\left[-\left(\frac{\varepsilon - k''}{a}\right)^m\right] + \mu(\sigma_2 + \sigma_3), (\varepsilon \geqslant k'') \end{cases} \tag{19}$$

where

$$E = -0.60M^3 + 29.75M^2 - 509.70M + 4068.47$$

$$k'' = -0.0248\sigma_3 + (-0.028M + 0.88)$$

Using the model developed in this study, the theoretical curves of stress-strain relationship are obtained and compared with the experimental curves, as shown in Fig. 11. The model can accurately describe the linear elastic characteristics of crumb rubber mortars undergoing small deformation and nonlinear mechanical behavior after the point of peak strength. The complete process of strain softening deformation of crumb rubber mortars obtained by this model is in good agreement with the experimental curves. Therefore, the model is reasonable and practical.

5. Conclusions

In this study, crumb rubber mortars with different rubber particle contents are prepared, and physical and mechanical experiments are conducted. Based on the Lemaitre equivalent strain theory of rock damage, by incorporating the influence of the damage threshold of crumb rubber mortars, the damage evolution model of crumb rubber mortars and the damage constitutive model of crumb rubber mortars are discussed for the entire process of simulating the strain softening deformation. The following conclusions can be drawn.

(1) The stress-strain curves of crumb rubber mortars obtained from experiments show that the peak strength of the rubber particles decreases as the rubber particle content increases. After the peak strength is reached, the strain softening property decreases gradually, and the elastic modulus decreases exponentially. The Poisson's ratio shows dynamic variation. Before the peak strain, this parameter increases linearly. After the peak strain, it increases logarithmically.

(2) A damage constitutive model of crumb rubber mortars considering the effect of damage threshold is established that can accurately describe the stress-strain relationship of crumb rubber mortars with various rubber contents under triaxial compression state. Relative to the experimental results, the model in this paper can accurately describe the entire process of the strain softening deformation of crumb rubber mortars under a complex stress state.

(3) The range of the value of damage threshold, k, is discussed. The damage threshold, k, of CRC is generally between 0.1 and 0.9. The lower the rubber particle content, the lower the confining pressure and the greater the damage threshold. When the confining pressure increases from 0 MPa to 5 MPa, the damage threshold decreases sharply. When the confining pressure increases from 5 MPa to 10 MPa, the damage threshold exhibits a smaller variation relative to the former response, indicating that the damage threshold is more sensitive in the initial stage of the confining pressure.

Conflict of interest

We declare that we have no potential conflict of interest.

Acknowledgments

This research was funded by the National Key Research and Development Program, China (Grant No. 2016YFC0600902), the National Natural Science Foundation of China, China (Grant Nos. 51474135 and 51774192), and the Natural Science Foundation of Shandong Province, China (Grant No. ZR201702180216). This support is greatly appreciated.

References

[1] L.-J. Hunag, H.-Y. Wang, S.-Y. Wang, A study of the durability of recycled green building materials in lightweight aggregate concrete, Constr. Build. Mater. 96 (2015) 353–359.
[2] M. Nehdi, A. Khan, Cementitious composites containing recycled tire rubber: an overview of engineering properties and potential applications, Cem. Concr. Aggreg. 23 (1) (2001) 3–10.
[3] G. Long, N. Li, Y. Xue, Y. Xie, Mechanical properties of self-compacting concrete incorporating rubber particles under impact load, J. Chin. Ceram. Soc. 44 (8) (2016) 1081–1090.
[4] Kunal Bisht, P.V. Ramana, Evaluation of mechanical and durability properties of crumb rubber concrete, Constr. Build. Mater. 155 (2017) 811–817.
[5] Y. Yu, H. Zhu, Influence of rubber size on properties of crumb rubber mortars, Materials 9 (7) (2016) 527.
[6] C.J. Waldron, T.E. Cousins, A.J. Nassar, J.P. Gomez, Demonstration of use of high-performance lightweight concrete in bridge super structure in Virginia, J. Perform. Constr. Facil. 19 (2) (2005) 146–154.
[7] F. Hernández-Olivares, G. Barluenga, B. Parga-Landa, M. Bollatid, B. Witoszek, Fatigue behaviour of recycled tyre rubber-filled concrete and its implications in the design of rigid pavements, Constr. Build. Mater. 21 (10) (2007) 1918–1927.
[8] T. Gupta, S. Chaudhary, R.K. Sharma, Assessment of mechanical and durability properties of concrete containing waste rubber tire as fine aggregate, Constr. Build. Mater. 73 (2014) 562–574.
[9] N. Ganesan, J.R. Bharati, A.P. Shashikala, Flexural fatigue behavior of self compacting rubberized concrete, Constr. Build. Mater. 44 (2013) 7–14.
[10] A.C. Ho, A. Turatsinze, R. Hameed, D.C. Vu, Effects of rubber aggregates from grinded used tyres on the concrete resistance to cracking, J. Clean. Prod. 23 (1) (2012) 209–215.
[11] L.-J. Li, Z.-Z. Chen, W.-F. Xie, F. Liu, Experimental study of recycled rubber-filled high-strength concrete, Mag. Concr. Res. 61 (7) (2009) 549–556.
[12] W. Shen, L. Shan, T. Zhang, H. Ma, Z. Cai, H. Shi, Investigation on polymer-rubber aggregate modified porous concrete, Constr. Build. Mater. 38 (2013) 667–674.
[13] A.R. Khaloo, M. Dehestani, P. Rahmatabadi, Mechanical properties of concrete containing a high volume of tire-rubber particles, Waste. Manage. 28 (12) (2008) 2472–2482.
[14] F. Liu, L.-Y. Meng, G.-F. Ning, L.-J. Li, Fatigue performance of rubber-modified recycled aggregate concrete (RRAC) for pavement, Constr. Build. Mater. 95 (2015) 207–217.

[15] L. Li, S. Ruan, L. Zeng, Mechanical properties and constitutive equations of concrete containing a low volume of tire rubber particles, Constr. Build. Mater. 70 (2014) 291–308.
[16] H. Zhang, M. Gou, X. Liu, X. Guan, Effect of rubber particle modification on properties of rubberized concrete, J. Wuhan. Univ. Technol. 29 (4) (2014) 763–768.
[17] H. Su, J. Yang, T.-C. Ling, G.S. Ghataora, S. Dirar, Properties of concrete prepared with waste tyre rubber particles of uniform and varying sizes, J. Clean. Prod. 91 (2015) 288–296.
[18] W. Feng, Y. Wei, L. Li, F. Liu, Y. Chen, Experimental study on constitutive equation of high strength crumb rubber concrete to uniaxial compression, New. Build. Mater. 2 (2010) 12–15.
[19] A.F. Angelin, R.C. Cecche Lintz, L.A. Gachet-Barbosa, W.R. Osório, The effects of porosity on mechanical behavior and water absorption of an environmentally friendly cement mortar with recycled rubber, Constr. Build. Mater. 151 (2017) 534–545.
[20] A.F. Angelin, M.F.F. Andrade, R. Bonatti, R.C. Cecche Lintz, L.A.G. Barbosa, W.R. Osório, Effects of spheroid and fiber-like waste-tire rubbers on interrelation of strength-to-porosity in rubberized cement and mortars, Constr. Build. Mater. 95 (2015) 525–536.
[21] H. Xiong, M.-F. Fu, Q.-F. Luo, A new subsection curve damage model of concrete, Chin. Q. Mech. 25 (3) (2004) 343–348.
[22] J. Lemaitre, A continuous damage mechanics model for ductile fracture, J. Mater. Sci. Technol. 107 (1985) 83–89.
[23] W. Cao, H. Zhao, L. Zhang, Y. Zhang, Damage statistical softening constitutive model for rock considering effect of damage threshold and its parameters determination method, Chin. J. Rock. Mech. Eng. 27 (6) (2008) 1148–1154.
[24] Y.-L. Xue, S.-L. Li, F. Lin, H.-B. Xu, Study of damage constitutive model of SFRC considering effect of damage threshold, Rock. Soil. Mech. 30 (7) (2009) 1987–1999.
[25] W.-G. Cao, X. Li, A new discussion on damage softening statistical constitutive model for rocks and method for determining its parameters, Rock. Soil. Mech. 29 (11) (2008) 2952–2956.
[26] S.-Q. Yang, W.-Y. Xu, L.-D. Wei, C.-D. Su, Statistical constitutive model for rock damage under uniaxial compression and its experimental study, J. Hohai. Univ. 32 (2) (2004) 200–203.
[27] S.-C. Li, J. Xu, K.-G. Li, Y.-Q. Tao, X.-J. Tang, Study on damages constitutive model of rocks based on Weibull distributing, J. Hunan. Univ. Sci. Technol. 22 (4) (2007) 65–68.
[28] R. Cao, S. He, J. Wei, F. Wang, Study of modified statistical damage softening constitutive model for rock considering residual strength, Rock. Soil. Mech. 34 (06) (2013). 1652–1660+1667.
[29] S. Liu, C. Liu, X. Han, L. Cao, Weibull distribution parameters of rock strength based on multi-fractal characteristics of rock damage, Chin. J. Geotech. Eng. 33 (11) (2011) 1786–1791.